Colloids and Surfaces A: Physicochem. Eng. Aspects 348 (2009) 64–69

Contents lists available at ScienceDirect

Colloids and Surfaces A: Physicochemical and Engineering Aspects

journal homepage: www.elsevier.com/locate/colsurfa

Phase transitions in Langmuir monolayer of long chain attached fluorescein studied by second harmonic generation technique

Héctor Gutiérrez[a], Lorenzo Echevarria[b], Manuel Caetano[a,*]

[a] Universidad Central de Venezuela, Escuela de Química, Ofic. 022, P.O. Box 47102, Caracas 1080-A, Venezuela
[b] Universidad Simón Bolívar, Departamento de Química, P.O. Box 89000, Caracas 1080-A, Venezuela

ARTICLE INFO

Article history:
Received 26 January 2009
Received in revised form 19 June 2009
Accepted 23 June 2009
Available online 1 July 2009

Keywords:
Langmuir monolayers
Phase transition
Second harmonic generation
Liquid–gas interfaces

ABSTRACT

Optical second harmonic generation (SHG) measurements coupled with Π-A isotherms have been shown to be helpful, for the following and comprehension of orientational orders and phase transitions in Langmuir monolayers. Using the SHG-(Π-A) measurements, monolayers of 5-hexadecanoylaminofluorescein on the water surface were examined by monolayer compression. The phase transitions were noticeably revealed. Dependence of the square root of the intensities polarizations quotient in the molecules surface density, allowed establishing tilting orientation alignment phases. In addition, change in the monolayer symmetry $C_{\infty v} \rightarrow C_{2v}$ as it goes through the LE–LC phase transition, was clearly recognized. It was concluded that a possible change in β is taking place due to aggregate formation.

1. Introduction

Insoluble monolayers of large amphiphile molecules possessing long hydrocarbon chains spread at the air/water interface possess an extraordinary diversity of phases and a remarkable wealth of structures. The main transitions characterized by the coexistence between phases such as the G – gaseous, LE – liquid expanded, LC – liquid condensed, S – solid, usually are determined from the (Π-A) isotherm of the layer [1,2]. However, this standard method does not work for the continuous liquid condensed–solid and orientational transitions.

Regardless of considerable research on these systems, our present knowledge of the physical chemistry of these Langmuir monolayers is still partial. While the unique geometry of the air–water interface has allowed for measurements of some macroscopic properties of these, there is a significant lack of knowledge about intermolecular interactions and lateral organization in the films. Since the molecules are flexible to some extent, the difficulty lies in how to experimentally determine both the orientational angle and angular distribution of particular sections or parts of the molecules in the film. Knowledge about both orientational angle and angular distribution is important for many molecular monolayers or films, even a rough estimation of angular distribution permit, sometimes, the characterization of their properties.

Recently, a variety of experimental techniques coupled with Π-A isotherm measurement have been developed for exploring the structure of monolayers. Spectroscopic techniques with submonolayer sensitivity are extremely valuable in terms of investigation of such complexity of molecular monolayer.

Second harmonic generation (SHG) has been developed in the last decade as a powerful technique for probing the orientational ordering of molecules physically or chemically deposited onto interfaces, providing information at the fundamental level [3–9]. The reason the SHG can probe selectively the interface between to media without being overwhelm by the response of the species present in the bulk, is that the SHG is a second-order optical process and thus forbidden by symmetry reasons in isotropic or centrosymmetric media [10,11]. Due to its optical nature, this technique can have access to embedded interfaces if the bulk media are transparent. Besides, because it is a non-invasive technique, requiring no physical contact with interface, it has allowed probing in situ the process occurring in the interface.

In the present paper, a second harmonic generation (SHG) technique, coupled with simultaneously measure of (Π-A) isotherms, has been applied in order to determine the phase transitions in a monolayer of a fluorescein dye at the air–water interface. We also present an innovative and quantitative analysis strategy for surface SHG data, which provides detailed information for understanding the physical picture of Langmuir monolayer.

1.1. Theory of SHG in interfaces

Second harmonic generation (SHG), from insoluble films of an amphiphile at the air–water interface, can be thought of as coming

* Corresponding author. Tel.: +58 212 6051216; fax: +58 212 6051246.
E-mail address: manuel.caetano@ciens.ucv.ve (M. Caetano).

0927-7757/$ – see front matter © 2009 Elsevier B.V. All rights reserved.
doi:10.1016/j.colsurfa.2009.06.034

from a polarization sheet created by the interaction between the incident radiation and the molecules adsorbed in the interface. The SHG can be depicted in terms of the second-order non-linear polarization sheet, $\mathbf{P}^{(2)}(2\omega)$, induced by the fundamental radiation, $\mathbf{E}(\omega)$, striking the interface with the fundamental frequency ω:

$$\mathbf{P}^{(2)}(2\omega) = \chi^{(2)}(2\omega)\mathbf{E}(\omega)\mathbf{E}(\omega) \tag{1}$$

where $\chi^{(2)}(2\omega)$ is known as the non-linear second-order electric susceptibility. $\chi^{(2)}$ is a third rank tensor and determine completely the second-order non-linear optical response of the interface.

1.1.1. Monolayer symmetry

Assuming that the adsorbed monolayer is isotropic and lays on the xy plane ($C_{\infty v}$ symmetry), $\chi^{(2)}$ reduce to [12]:

$$\chi^{(2)} = \begin{bmatrix} 0 & 0 & 0 & 0 & \chi_{xzx} & 0 \\ 0 & 0 & 0 & \chi_{xzx} & 0 & 0 \\ \chi_{zxx} & \chi_{zyy} & \chi_{zzz} & 0 & 0 & 0 \end{bmatrix} \tag{2}$$

where additionally $\chi_{zxx} = \chi_{zyy}$ and $\chi_{xzx} = \chi_{yzy}$. Thus in this case the tensor has only three independent components.

From the solution of the Maxwell equations, using as source the non-linear polarization sheet it is obtained the following relation between the SHG field, $\mathbf{E}(2\omega)$, and the incident field, $\mathbf{E}(\omega)$, for the $C_{\infty v}$ symmetry [12,13]:

$$\begin{aligned} E_p(2\omega) &= a_{ppp}E_p^2(\omega) + a_{pss}E_s^2(\omega) \\ E_s(2\omega) &= a_{sps}E_p(\omega)E_s(\omega) \end{aligned} \tag{3}$$

where the subindexes p and s stand for field's polarizations parallel and normal to the plane of incidence respectively, and:

$$\begin{aligned} a_{ppp} &= 8\pi ik[2F_x\chi_{xzx}\cos\theta_{inc}\sin\theta_{inc} \\ &\quad + F_z(\chi_{zxx}\cos^2\theta_{inc} + \chi_{zzz}\sin^2\theta_{inc})] \\ a_{pss} &= 8\pi ikF_z\chi_{zyy} \\ a_{sps} &= 16\pi ikF_y\chi_{yzy}\sin\theta_{inc} \end{aligned} \tag{4}$$

where F_x, F_y and F_z are related to the Fresnell's factors for the interface [13,14].

If the monolayer has a symmetry C_{2v}, i.e. molecules align themselves along some direction in the plane of the monolayer, $\chi^{(2)}$ has also the form shown in Eq. (2), but in this case $\chi_{zxx} \neq \chi_{zyy}$ and $\chi_{xzx} \neq \chi_{yzy}$ [10,11]. However, the SHG field has exactly the same form of Eq. (3). This means that, experimentally, it is not always easy to distinguish between both types of monolayer symmetry.

$\chi^{(2)}$ is a macroscopic quantity, but can be related to the microscopic properties of the molecules forming the interface (monolayer) by the expression:

$$\chi^{(2)} = N_s l(\omega, 2\omega)\langle\beta R(\phi, \theta, \psi)\rangle_{av} \tag{5}$$

where N_S is the molecules surface density, $l(\omega, 2\omega)$ is a factor that depicts local field corrections, β is the second-order molecular polarizability or first hyperpolarizability, R is a matrix that depicts the coordinate transformation from the molecular coordinates system (x', y', z'), to the laboratory coordinates system (x, y, z), by mean of the Euler's angles (ϕ, θ, ψ), and the brackets means the average over all possible molecular orientations in the interface. The Euler's angles are defined so that θ is the angle between the z-and z'-axes.

The hyperpolarizability of the Fluorescein H-110 is governed by the optical response of the system of π-electrons of the fluorescein chromophore, especially by the strong absorption band at 490 nm. This band is assigned to the $S_0 \rightarrow S_1$ transition [15], which has a transition dipolar moment lying in the plane of the xantene moiety, along the molecular z'-axis [16]. This leads to a beta with a dominant $\beta_{z'z'z'}$ component. Thus, neglecting the contribution of the others more weak components we can write the relation between the components of χ and β as

$$\begin{aligned} \chi_{zzz} &= N_S l_{zz}^2(\omega)l_{zz}(2\omega)\beta_{z'z'z'}\langle\cos^3\theta\rangle \\ \chi_{zyy} &= \frac{1}{2}N_S l_{yy}^2(\omega)l_{zz}(2\omega)\beta_{z'z'z'}\langle\cos\theta\sin^2\theta\rangle \\ \chi_{yzy} &= \frac{1}{2}N_S l_{zz}(\omega)l_{yy}(\omega)l_{yy}(2\omega)\beta_{z'z'z'}\langle\cos\theta\sin^2\theta\rangle \end{aligned} \tag{6}$$

So, by obtaining the components of χ from measurement of SHG, we can in turn obtain some estimation of the mean orientation of the fluorescein moiety of the molecules in the interface.

2. Experimental

2.1. Preparation of Fluorescein H-110 (5-hexadecanoylaminofluorescein) monolayer

A home-built Langmuir trough made in Teflon was extensively cleaned and then filled with ultrapure water. The trough was fastened to a vibration isolated optical table. 5-Hexadecanoylaminofluorescein, a lipophilic dye Fluorescein H-110 from molecular probes was dissolved in a mixture of ethanol and chloroform HPLC grade to obtain a 10^{-4} M solution. Subsequently, 60 μL of this solution was taken with a Hamilton microliter syringe and placed on the water surface, where the chloroform was allowed to evaporate. A Teflon barrier, driven by a motorized translation stage Newport-Klinger, Irvine, CA, and running linearly along the top edge of the trough was used to control the surface area available to the monolayer. Compression of the surface was made at a rate of 5 mm min^{-1}. Surface pressure was measured using a tailor-made optical Wilhelmy balance [17].

2.2. SHG setup

Fig. 1 shows the experimental setup. The source is a Nd:YAG pulsed laser (Continuum, model Surelite I) that emits nanosecond pulses at 1064 nm with a energy per pulse of 10 mJ. A small fraction of the laser radiation was separated by a beam splitter, attenuated by a neutral density filter, and directed to a photodetector to provide a reference signal. In order to have absolute energy calibration of the photodetector, a pulse energy detector (MOLECTRON) was placed at the monolayer position with all the optics in place and a calibration curve of the incident energy (mJ) versus the reference signal (mV) was obtained. The main laser beam goes through a set of filters that remove wavelengths other than 1064 nm and then is focused on the interface. The polarization of the incident pulses is controlled with a half-wave plate. The transmitted SHG radiation is directed to a Glan–Thompson polarizer to select the desired component before arriving at the detection system. A system of filters are arranged at the exit of the polarizer to eliminate any residual fundamental radiation that may contaminate the SHG signal, which is detected by a Hammamatsu R955 photomultiplier tube (PMT), in a small monochromator and averaged in a boxcar (Stanford Research Instruments, SR 250).

Calibration of the PMT was carried out using the Nd:YAG laser at 532 nm. A known portion of the laser output energy

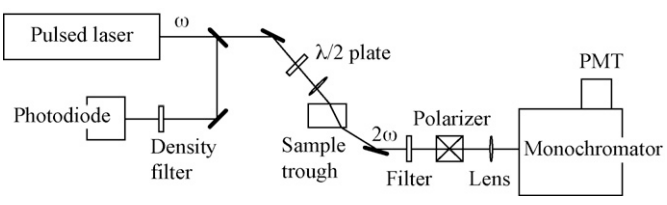

Fig. 1. The experimental setup for SHG measurement in transmission.

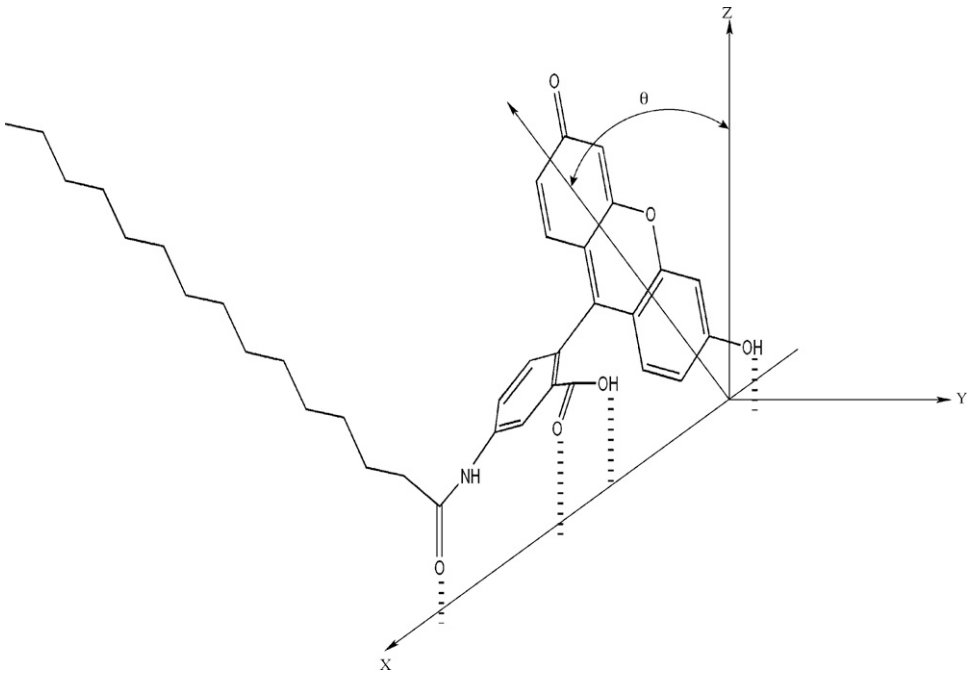

Fig. 2. Chemical formula of 5-hexadecanoylaminofluorescein (Fluorescein H-110) and the experimental geometry and coordinates. The coordinate (*X*, *Y*, *Z*) is fixed to the sample trough. The compression direction was the *Y*-axis.

is directed into an energy meter by means of a beam splitter. The rest of the light was attenuated and directed onto the monochromator–photomultiplier combination. A calibration curve allows for conversion of PMT signal (mV) into absolute energy (mJ).

2.3. Experimental geometry

As is shown in Fig. 2, the monolayer coincides with the *x*–*y* plane, and the plane of incidence is the *x*–*z* plane; the direction of compression was along the *y*-axis. The intensity of the second harmonic radiation generated were measured with the combination of ingoing fundamental and outgoing SHG polarizations shown in Table 1.

3. Results and discussion

3.1. Surface pressure-area (Π-*A*) isotherm and SHG intensities in Fluorescein H-110 monolayer

The monolayer was compressed step by step at 21 °C, reducing the same amount of area in each step. The area was held constant about 3 min, to assure steady state, and then Π and SHG were simultaneously measured and recorded against area by molecule. The observed Π-A isotherm is shown in Fig. 3. The features of the isotherm may be interpreted in terms of four monolayer phases: gas, liquid-expanded (LE), liquid-condensed (LC), and solid [18–20]. At large available areas (>70 Å^2 per molecule) the monolayer is in the gas state. At ~70 Å^2 per molecule an approximately horizontal region in the isotherm is reached indicating the gas–LE transition. In this region the hydrophobic tail groups, which were originally lying almost flat on the water surface, are subsequently being lifted from that surface. At 48 Å^2 per molecule the compressibility approaches infinity, indicating a first-order phase transition from the LE to the LC phase. At a surface area of just over 38 Å^2 per molecule there is an abrupt increase of slope. This is due to a phase change and represents a transition to an ordered arrangement of the molecules, known as the solid condensed or solid phase. If this second linear portion of the isotherm is extrapolated to zero surface pressure, the intercept gives an area per Fluorescein H-110 molecule of 43 Å^2; that would be expected for the hypothetical state of an uncompressed close-packed layer [21].

I_{pp} and I_{qs} SHG intensities versus area are also plotted in Fig. 3. Both intensities curves follow the same pattern than the Π-A isotherm, showing that phase changes are reflected in the monolayer non-lineal optical response. Between 53 and 38 Å^2, a plateau region specifies the coexistence range of a first-order phase transition, LE–LC [21].

Table 1
Nomenclature for SHG polarizations.

SHG Intensity	Ingoing polarization	Outgoing polarization
I_{pp}	*p*	*p*
I_{ps}	*p*	*s*
I_{qs}	45°	*s*
I_{ss}	*s*	*s*

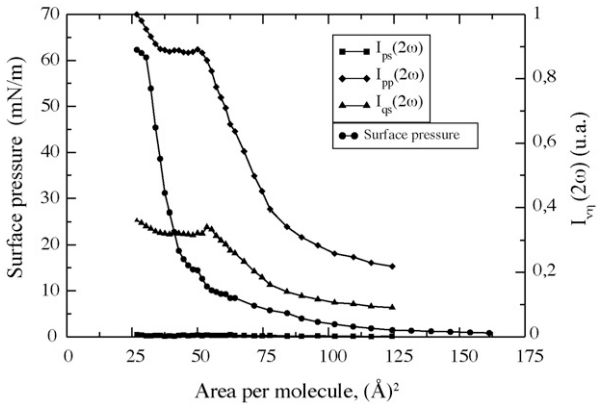

Fig. 3. Π-A isotherms and ν polarized input and η polarized output light second harmonic intensity spectra ($I_{\nu\eta}$) versus area.

It is clearly noticeable that intensities I_{ss} and I_{ps} are not detectable trough all the compression; therefore the monolayer has a C_n symmetry axis normal to the plane surface. It can be assumed that, at least in the gas region, the monolayer is isotropic corresponding to a $C_{\infty v}$ symmetry. The non-linear optical susceptibility $\chi^{(2)}$ therefore have only three independent components, χ_{zzz}, $\chi_{yzy} = \chi_{xzx}$, $\chi_{zyy} = \chi_{zxx}$. However, obeying to the compression and the restricted symmetry of a bidimensional system, it is possible that the monolayer is condensing in an ordered structure, while is suffering some of the phase transitions observed in the isotherm [15,22–24]. Additionally, C_{2v} symmetry is congruent with an anisotropy imposed over the monolayer, through plane direction during compression. Hence, a $C_{\infty v} \rightarrow C_{2v}$ transition of the interface symmetry has to be considered. However, since $I_{ss} = I_{ps} = 0$ in both cases, additional experimental data and analysis is necessary to make a distinction between both symmetries.

3.2. SHG intensities analysis

As was mentioned in the previous section, I_{pp} and I_{qs} intensities follow, in general, the same behavior. However, differences are present in the relative slopes, particularly after entering the LC region. These differences indicate that the monolayer is undergoing a change in its optical response, higher than would be expected from the simple effect of the increase in molecular number density due to the compression [22,23]. As was mentioned before, the monolayer molecules could exhibit a change of symmetry occasioned by the compression. This can be better observed in Fig. 4a, where $\sqrt{I_{pp}}$ and $\sqrt{I_{qs}}$ are plotted versus the molecular surface density (N_S) in

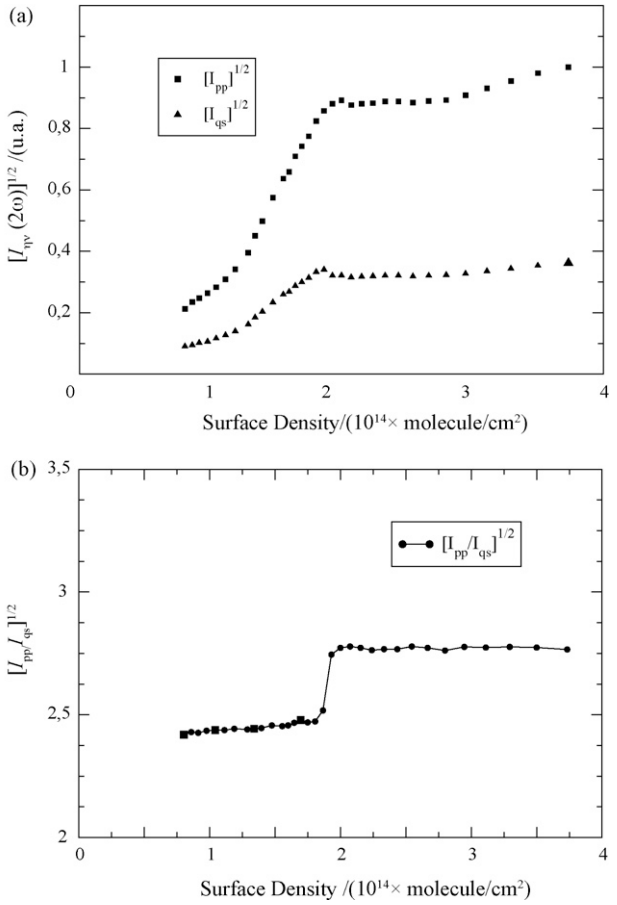

Fig. 4. (a) Square root of the I_{pp} and I_{qs} SHG intensities versus molecular surface density N_S. (b) Square root of the I_{pp} and I_{qs} SHG intensities quotient versus molecular surface density N_S.

the monolayer. If we can assume an isotropic distribution in the interface plane, then:

$$\sqrt{I_{pp}} \propto r_p(\langle\theta\rangle)\beta_{z'z'z'}N_S,$$
$$\sqrt{I_{qs}} \propto r_q(\langle\theta\rangle)\beta_{z'z'z'}N_S \quad (7)$$

where $r_p(\langle\theta\rangle)$ and $r_q(\langle\theta\rangle)$ are functions of the mean orientation angle respect to the surface normal, we can conclude that this relation is lineal only if both $r_j(\langle\theta\rangle)$ and $\beta_{z'z'z'}$ are independent from N_S.

At low molecular densities, in the G phase, both square root intensities follow a linear behavior that extrapolate approximately to zero, being consistent with Eq. (7), this means that neither the molecular orientation nor beta changes with the compression in this region. In the LE phase transition region the curves suffer a marked slope change, and yet it still follows a linear increase. At the LE–LC transition region the curves become more complicated than a simple linear function, obeying to an expected change in the monolayer symmetry.

To take a deeper insight of this behavior, square root of I_{pp} and I_{qs} quotient can be obtained from Eqs. (3) and (4), and expressed as

$$\sqrt{\frac{I_{pp}}{I_{qs}}} = \left| \left(\frac{F_x}{F_y} + \frac{1}{2}\frac{F_z}{F_y} \right) \frac{\chi_{xzx}}{\chi_{yzy}} + \frac{1}{2}\frac{F_z}{F_y}\frac{\chi_{zzz}}{\chi_{yzy}} \right| \quad (8)$$

where the explicit dependence in N_S has been eliminated, thus the only dependence in N_S would be implicit in $\langle\theta\rangle$. This quotient was plotted as a function of N_S as shown in Fig. 4b. It is clear that $\sqrt{(I_{pp}/I_{qs})}$ has almost no dependence with N_S, with the evident exception of the step occurring around the LE–LC phase transition (when $N_S \sim 2 \times 10^{14}$ mol cm^{-2}). This result is overly interesting and indicates two things. Firstly, the molecular orientation with respect to the surface normal has a very small change through the whole compression process. This is clearly evident in the fact that the curve has a very flat slope along the whole measurement interval, indicating no change in $\langle(\theta)\rangle$. Secondly, the step in the curve at $N_S \sim 2 \times 10^{14}$ mol cm^{-2} indicates a change of symmetry in the monolayer as it undergoes the LE–LC phase transition. This symmetry change is due to the forced reordering induced by the compression. All the information about this symmetry change is contained in the first term of Eq. (8).

3.3. Polarization spectra and $\chi^{(2)}$ calculations

Once the SHG field passes through a polarizer rotated by an angle ψ with respect to its principal axis, it can be written as

$$E_\psi(2\omega) = E_p(2\omega)\cos(\psi) + E_s(2\omega)\sin(\psi) \quad (9)$$

and its intensity, relative to the intensity of the incident radiation, $E(\omega)$:

$$R_\psi = \frac{|E_\psi(2\omega)|^2}{|E(\omega)|^4} \quad (10)$$

Rotating the half-wave plate in an angle φ sets the polarization angle of the fundamental incident radiation. After passing through the retarding device, the incident electric field polarized in the p and s direction has the following components:

$$E_p(\omega) = E(\omega)\ \cos(2\varphi),$$
$$E_s(\omega) = E(\omega)\sin(2\varphi) \quad (11)$$

If the analyzer (Glan–Thompson) is set to detect SH radiation with p or s polarization ($\psi = 0$ or $\psi = 90$), we can obtain, using Eqs. (10) and (11):

$$R_p(\varphi) = |a_{ppp}\ \cos^2(2\varphi) + a_{pss}\sin^2(2\varphi)|^2,$$
$$R_s(\varphi) = |a_{sps}\sin(2\varphi)\ \cos(2\varphi)|^2 \quad (12)$$

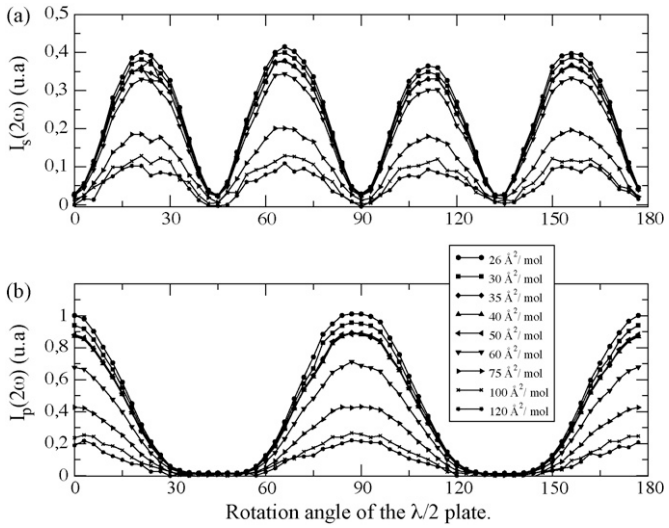

Fig. 5. (a) SH intensity $I_s(2\omega)$ and (b) SH intensity $I_p(2\omega)$ versus polarization angle from different monolayer compression stages. Fourfold and eightfold symmetries for $I_p(2\omega)$ and $I_s(2\omega)$, respectively, are present.

Polarization spectra of $I_p(2\omega)$ and $I_s(2\omega)$ signals from different monolayer compression states are shown in Fig. 5. Fourfold and eightfold symmetries for I_p and I_s curves, respectively, are clearly observed, as is expected from a monolayer with C_{2v} or $C_{\infty v}$ symmetry axis. Curve fitting analysis of these data, using as model Eq. (12), gave the absolute values of the components of the non-linear optical susceptibility tensor [12,25]. The respective values are shown in Table 2. Although the second harmonic frequency is not quite far from resonance, absorption at that frequency is negligible according to the respective absorption spectra. Therefore, it can be assumed that all susceptibilities are real.

If we suppose that in the G and LE phases the monolayer is isotropic (symmetry $C_{\infty v}$) then $\chi_{xzx} = \chi_{yzy}$. When the molecules in the monolayer rearrange themselves to a C_{2v} symmetry then $\chi_{xzx} \neq \chi_{yzy}$ and the first term of the right side of Eq. (8) changes abruptly its value. This is one of the reasons that the curve in Fig. 4b has a step in the transition LE–LC. This symmetry change does not affect the orientation along the surface normal, because the compression simply induces the molecules to align in the plane of the monolayer, without affecting the inclination respect to the normal. More specifically, as the compression is normal to the plane of incidence, and curve increases after the change of symmetry, then χ_{xzx} must increase respect to χ_{yzy}. Thus the molecules trend to align along the *x*-axis, normal to the direction of compression.

3.4. Molecular orientation measurements

The mean tilt angle of the molecular dipole with the interface normal, $\langle\theta\rangle$, was determined from the theoretical evaluation of β and the experimental values of the components of $\chi^{(2)}$ [26,27] for each stage of the monolayer compression process. As is shown in Table 3, $\langle\theta\rangle$ values change little during the compression course, from 54° at G phase to 50° at LE phase. Besides, the width of the angle distribution was determined following the procedure described in Ref. [26], and it scarcely decreases from 8° to 6° in the same compression range. An estimated of $\langle\theta\rangle$ during and after LE–LC transition becomes difficult due to the change in β. However, congruently with the argument derived from Fig. 4, an angle of 50° with respect of the surface normal can be assumed for the LC and S phases, by using the value obtained at 50 Å^2 (LE phase).

Table 2
Components of ($\chi^{(2)}/10^{-13}$ e.s.u.) at different compression stages.

Area/molecule	χ_{zzz}	χ_{yzy}	χ_{xzx}
120	0.131	0.107	0.107
100	0.169	0.138	0.138
75	0.291	0.222	0.222
60	0.543	0.359	0.359
50	0.585	0.370	0.370
40	0.594	0.372	0.483
35	0.645	0.381	0.495
30	0.683	0.407	0.529
26	0.736	0.424	0.551

Table 3
Mean tilt angle of the molecular dipole with the interface normal and full width at half maximum values for the angular distribution, at different compression stages.

Area/molecule	$\langle\theta\rangle$	FWHM
120	54 ± 1	8°
100	53 ± 1	8°
75	52 ± 1	7°
60	50 ± 1	6°

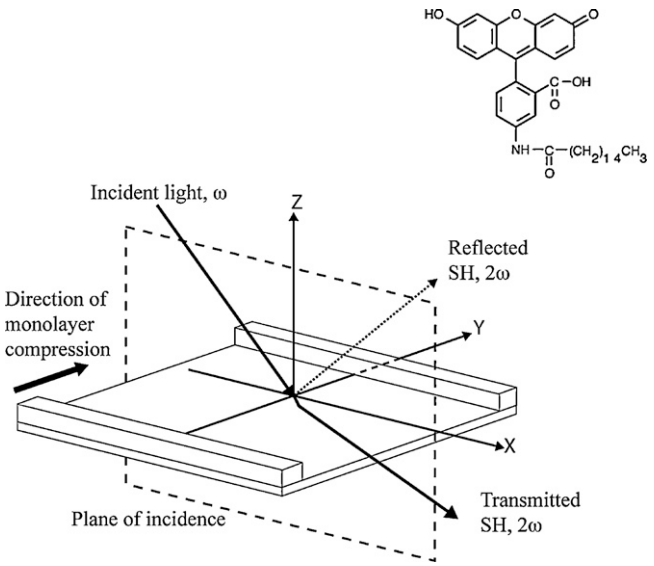

Fig. 6. A schematic diagram of the orientation of the Fluorescein H-110 molecule at the air/water interface (explanations for the angles are given in the text).

It has been reported that molecules with large π-conjugated systems capable of forming intermolecular charge-transfer, acquire a well defined out of plane orientation at the moment that the monolayer is spread over the interface [23,28–30]. The absence of any orientational variation during compression indicates that $\langle\theta\rangle$ is basically determined by structural features of the molecule and polar properties of the interface [21,31]. In the particular case of Fluorescein H-110, hydrogen bond formation between polar groups like –COOH, –CNHO, –OH, and water molecules on the surface determines the off-plane orientation, with the polar groups pointing to water and the long aliphatic chain pointing to air. Thus, xanthene ring is practically forced to acquire a $\langle\theta\rangle$ angle of about 50° as is shown in Fig. 6. By other hand, fluorescein molecules display a tendency to aggregate over time and under certain conditions. Compression at the confining air–water interface can yield aggregate formation and the corresponding change in β [15,32]. Consequently, the lack of linearity in $\sqrt{I_{pp}}$ would be attributed to a change in β due to aggregate formation rather than a change in $\langle\theta\rangle$.

4. Conclusions

In conclusion, optical second harmonic generation (SHG) measurements coupling with Π-A isotherms have clearly been shown

to be suitable for the determination of phase transitions, of the insoluble large amphiphile molecules possessing long hydrocarbon chains films at the air–water interface. Results obtained from SHG signal dependencies on area per molecule are in good agreement with those of (Π-A) isotherms. The use of $\sqrt{I_{pp}/I_{qs}}$ dependence on N_S allowed confirming, in a very easy way, that the molecular orientation with respect of the surface normal of the Fluorescein H-110 molecules in a Langmuir monolayer at the air–water interface, suffers a very little change through the whole compression process. Additionally, change in the monolayer symmetry $C_{\infty v} \rightarrow C_{2v}$ as it goes through the LE–LC phase transition, can be clearly observed from the same dependence. It can be concluded that a possible change in β is taking place due to aggregate formation.

Acknowledgements

This work was supported by grants from: FONACIT grant G-1997000593 and the CDCH Universidad Central de Venezuela grant PI-03.00.6691.2007.

References

[1] W.D. Harkins, T.F. Young, E. Boyd, The thermodynamics of films: energy and entropy of extension and spreading of insoluble monolayers, J. Chem. Phys. 8 (1940) 954–965.
[2] D.G. Dervichian, Changes of phase and transformations of higher order in monolayers, J. Chem. Phys. 7 (1939) 931–948.
[3] Y.R. Shen, Optical second harmonic generation at interfaces, Annu. Rev. Phys. Chem. 40 (1989) 327–350.
[4] Y.R. Shen, Surfaces probed by nonlinear optics, Surf. Sci. 299 (1994) 551–562.
[5] K.B. Eisenthal, Liquid interfaces probed by second harmonic and sum frecuency spectroscopy, Chem. Rev. 96 (1996) 1343–1360.
[6] D.C. Bain, Sum frequency vibrational spectroscopy of the solid/liquid interface, J. Chem. Soc., Faraday Trans. 91 (1995) 1281–1296.
[7] M. Iwamoto, A. Tojima, T. Manaka, O.Y. Zhong-can, Compression-shear-induced tilt azimuthal orientation of amphiphilic monolayers at the air–water interface: A $C_{\infty v} \rightarrow C_{2v}$ transition in the flow of a two-dimensional hexatic structure, Phys. Rev. E 67 (2003) 041711.
[8] A. Tojima, H. Fujimaki, T. Manaka, M. Iwamoto, Detection of phase transition of 4-alkoxy-4′-n-cyanobiphenyl Langmuir films by Maxwell displacement current and optical second-harmonic generation measurements, Thin Solid Films 438–439 (2003) 440–444.
[9] A. Tojima, T. Manaka, T. Manaka, M. Iwamoto, Orientational order study of monolayers at the air–water interface by Maxwell-displacement current and optical second harmonic generation, J. Chem. Phys. 115 (2001) 9010–9017.
[10] R.W. Boyd, Nonlinear Optics, Academic Press, San Diego, CA, 1992.
[11] Y.R. Shen, Principles of Nonlinear Optics, John Wiley & Sons, 1984.
[12] B.U. Felderhof, A. Bratz, G. Marowsky, O. Roders, F. Sieverdes, Optical second harmonic generation from adsorbate layers in total reflection geometry, J. Opt. Soc. Am. B: Opt. Phys. 10 (1993) 1824–1833.
[13] B.U. Felderhof, G. Marowsky, Linear optics of polarization sheets, Appl. Phys. B 43 (1987) 161–166.
[14] B.U. Felderhof, G. Marowsky, Electromagnetic radiation from a polarization sheet located at an interface between two media, Appl. Phys. B 44 (1987) 11–17.
[15] A.K. Dutta, C. Salesse, A spectroscopic and epifluorescence microscopic study of (hexadecanoylamino)fluorescein aggregates at the air–water interface and in Langmuir–Blodgett films, Langmuir 13 (1997) 5401–5408.
[16] J.P. Hermann, J. Ducuing, Dispersion of the two-photon cross section in rhodamine dyes, Opt. Commun. 6 (1972) 101–105.
[17] H.M. Gutierrez, J.A. Castillo, J.R. Chirinos, M. Caetano, Inexpensive Wilhelmy balance based in a fiber optic sensor for the study of Langmuir films, Rev. Sci. Instrum. 76 (2005) 045112.
[18] G.G. Roberts, Langmuir–Blodgett Films, Plenum, New York, 1990.
[19] C.M. Knobler, Condensed monolayer phases at the air/water interface: phase transitions and structures, J. Phys.: Condens. Matter (1991) S17.
[20] N.R. Pallas, B.A. Pethica, Liquid-expanded to liquid-condensed transition in lipid monolayers at the air/water interface, Langmuir 1 (1985) 509–513.
[21] G.L. Gaines, Insoluble Monolayers at Liquid–Gas Interfaces, John Wiley and Sons Ltd., New York, 1966.
[22] V. Tsukanova, A. Harata, T. Ogawa, Second-harmonic probe of pressure-induced structure ordering within long-chain fluorescein monolayer at the air/water interface, J. Phys. Chem. B 104 (2000) 7707–7712.
[23] V. Tsukanova, H. Lavoie, A. Harata, T. Ogawa, C. Salesse, Microscopic organization of long-chain rhodamine molecules in monolayers at the air/water interface, J. Phys. Chem. B 106 (2002) 4203–4213.
[24] N. Vranken, M. Van der Auweraer, F.C. De Schryver, H. Lavoie, P. Belanger, C. Salesse, Influence of molecular structure on the aggregating properties of thiacarbocyanine dyes adsorbed to langmuir films at the air–water interface, Langmuir 16 (2000) 9518–9526.
[25] L. Echevarria, P. Nieto, H. Gutiérrez, V. Mujica, M. Caetano, SHG of ultrathin films of metal porphyrins on BK7 glass in total internal reflection geometry: theory and experiments, J. Phys. Chem. B 107 (2003) 9332–9338.
[26] Y. Rao, Y. Tao, H. Wang, Quantitative analysis of orientational order in the molecular monolayer by surface second harmonic generation, J. Chem. Phys. 119 (2003) 5226–5236.
[27] J. Wang, S.M. Buck, M.A. Even, Z. Chen, Molecular responses of proteins at different interfacial environments detected by sum frequency generation vibrational spectroscopy, J. Am. Chem. Soc. 124 (2002) 13302–13305.
[28] K. Kajikawa, T. Anzai, H. Takezoe, A. Fukuda, S. Okada, H. Matsuda, H. Nakanishi, T. Abe, H. Ito, Second-harmonic generation in Langmuir and Langmuir–Blodgett films of a polymer with pendant chromophore, Chem. Phys. Lett. 192 (1992) 113–116.
[29] M.A. Mayer, T.K. Vanderlick, Calculation of shapes of dipolar domains in two dimensional films: effect of dipole tilt, J. Chem. Phys. (1995).
[30] H. Hsiung, G.R. Meredith, H. Vanherzeele, R. Popovitz-Biro, E. Shavit, M. Lahav, Ordering of two nitroaniline-terminated amphiphiles at the air–water interface studied by optical second harmonic, Chem. Phys. Lett. 164 (1989) 539–544.
[31] K.B. Eisenthal, Equilibrium and dinamic processes at interfaces by second harmonic and sum frequency generation, Ann. Rev. Phys. Chem. 13 (1992) 627–661.
[32] H. Nakahara, K. Fukuda, D. Moebius, H. Kuhn, Two-dimensional arrangement of chromophores in J aggregates of long-chain merocyanines and its effect on energy transfer in monolayer systems, J. Phys. Chem. 90 (1986) 6144–6148.